AQAMAN, a bisamidine-based inhibitor of toxic protein inclusions in neurons, ameliorates cytotoxicity in polyglutamine disease models

Received for publication, November 21, 2018, and in revised form, December 26, 2018 Published, Papers in Press, December 28, 2018, DOI 10.1074/jbc.RA118.006307

Huiling Hong[‡§1], Alex Chun Koon[‡§1], Zhefan Stephen Chen[‡§1], Yuming Wei[‡§], Ying An[‡§], Wen Li[§], Matthew Ho Yan Lau[¶], Kwok-Fai Lau[§], Jacky Chi Ki Ngo[§], Chun-Ho Wong[§], Ho Yu Au-Yeung[¶], Steven C. Zimmerman[‖], and Ho Yin Edwin Chan[‡§2]**

*From the [‡]Laboratory of Drosophila Research, [§]School of Life Sciences, Faculty of Science, **Gerald Choa Neuroscience Centre, Chinese University of Hong Kong, Shatin, N.T., Hong Kong SAR, China, the [¶]Department of Chemistry, University of Hong Kong, Pok Fu Lam Road, Hong Kong SAR, China, and the [‖]Department of Chemistry, University of Illinois at Urbana-Champaign, Urbana, Illinois 61801*

Edited by Joseph M. Jez

Polyglutamine (polyQ) diseases are a group of dominantly inherited neurodegenerative disorders caused by the expansion of an unstable *CAG* repeat in the coding region of the affected genes. Hallmarks of polyQ diseases include the accumulation of misfolded protein aggregates, leading to neuronal degeneration and cell death. PolyQ diseases are currently incurable, highlighting the urgent need for approaches that inhibit the formation of disaggregate cytotoxic polyQ protein inclusions. Here, we screened for bisamidine-based inhibitors that can inhibit neuronal polyQ protein inclusions. We demonstrated that one inhibitor, AQAMAN, prevents polyQ protein aggregation and promotes de-aggregation of self-assembled polyQ proteins in several models of polyQ diseases. Using immunocytochemistry, we found that AQAMAN significantly reduces polyQ protein aggregation and specifically suppresses polyQ protein–induced cell death. Using a recombinant and purified polyQ protein (thioredoxin–Huntingtin–Q46), we further demonstrated that AQAMAN interferes with polyQ self-assembly, preventing polyQ aggregation, and dissociates preformed polyQ aggregates in a cell-free system. Remarkably, AQAMAN feeding of *Drosophila* expressing expanded polyQ disease protein suppresses polyQ-induced neurodegeneration *in vivo*. In addition, using inhibitors and activators of the autophagy pathway, we demonstrated that AQAMAN's cytoprotective effect against polyQ toxicity is autophagy-dependent. In summary, we have identified AQAMAN as a potential therapeutic for combating polyQ protein toxicity in polyQ diseases. Our findings further highlight the importance of the autophagy pathway in clearing harmful polyQ proteins.

Polyglutamine (polyQ)[3] diseases are a group of diseases characterized by an unstable *CAG* repeat expansion in the coding region of the affected genes, which in turn produces abnormal proteins with long stretches of polyQ tracts (1, 2). This group of diseases include Huntington's disease (HD), spinal and bulbar muscular atrophy (SBMA), dentatorubral pallidoluysian atrophy, and a number of spinocerebellar ataxias, including Machado-Joseph disease (MJD, also known as SCA3) (1, 2). Toxic proteins with polyQ stretches have a tendency to aggregate and form neuronal inclusions (3). The accumulation of aggregated and misfolded proteins induces endoplasmic reticulum (ER) stress (4, 5), leading to neuronal dysfunction and cell death (6), which subsequently contributes to the pathogenesis of polyQ diseases, including HD (7), SBMA (8), and MJD (9).

When the ER is under stress from deleterious unfolded proteins, the unfolded protein response (UPR) pathway is activated in the cell to transduce appropriate signals from the cytoplasm to the nucleus, which in turn induces the expression of numerous molecular chaperones and folding enzymes for the ER to cope with the stress condition (10, 11). Apart from managing unfolded proteins, the UPR pathway is also closely related to autophagy, which is an essential catabolic mechanism involving the degradation of misfolded proteins and damaged organelles through the lysosomal pathway (12, 13). Accumulating evidence indicates that persistent ER stress in neurodegenerative diseases often results

This work was supported by the CUHK Vice-Chancellor's One-Off Discretionary Fund VCF2014011 and EC/2017/012, CUHK Lui Che Woo Institute of Innovative Medicine Grant 8303404, CUHK Gerald Choa Neuroscience Centre Grant 7105306, the Croucher Foundation, the Hong Kong Postgraduate Fellowship (HKPF), donations from the Hong Kong Spinocerebellar Ataxia Association 6903291, and National Institutes of Health Grant RO1 AR069645. The authors declare that they have no conflicts of interest with the contents of this article. The content is solely the responsibility of the authors and does not necessarily represent the official views of the National Institutes of Health.

This article contains Figs. S1–S4.

[1] These authors contributed equally to this work.

[2] To whom correspondence should be addressed: School of Life Sciences, Chinese University of Hong Kong, Shatin, N.T., Hong Kong SAR, China. Tel.: 852-3943-4021; Fax: 852-2603-7732; E-mail: hyechan@cuhk.edu.hk.

[3] The abbreviations used are: polyQ, polyglutamine; HD, Huntington's disease; SBMA, spinal and bulbar muscular atrophy; MJD, Machado-Joseph disease; ER, endoplasmic reticulum; UPR, unfolded protein response; PMSF, phenylmethylsulfonyl fluoride; DMEM, Dulbecco's modified Eagle's medium; EGFP, enhanced GFP; ICC, immunocytochemistry; ITC, isothermal titration calorimetry; BBB, blood–brain barrier; LDH, lactate dehydrogenase; qRT-PCR, quantitative real-time PCR; EK, enterokinase; ESI-MS, electrospray ionization–mass spectrometer; ddH_2O, double distilled H_2O; Trx, thioredoxin.

in long-term activation of autophagy and the UPR pathway in neurons, which are likely compensatory mechanisms to relieve the ER stress (14, 15). The disruption of UPR or autophagy causes inefficient clearance of the accumulated proteins, which in turn contributes to the progression of neurodegeneration and cell death (13, 14).

No cure for polyQ diseases is known, so new therapeutics aimed at disaggregating or inhibiting the formation of the abnormal polyQ protein inclusions are urgently needed. Bisamidine-based compounds are a type of soluble small molecules capable of binding nucleic acids (16, 17). In this study, we found that a bisamidine inhibitor, AQAMAN, can reduce polyQ protein aggregation and suppress polyQ protein–induced cell death. We demonstrated that AQAMAN can bind to soluble forms of polyQ proteins and disrupt preformed polyQ aggregation *in vitro*. Notably, feeding AQAMAN to *Drosophila* with expanded polyQ protein expression suppressed neurodegeneration *in vivo*. AQAMAN also suppressed ER stress in both cell culture and *Drosophila* models of polyQ diseases. We further demonstrated that AQAMAN's protective effect on cells is autophagic pathway-dependent.

In summary, AQAMAN is a potent bisamidine inhibitor that effectively reduces polyQ protein aggregation, which has significant therapeutic potentials for combating polyQ diseases.

Results

AQAMAN suppresses polyQ protein-induced cell death

Our previous work has demonstrated that by using rational design, a series of bisamidine inhibitors can be designed to bind to the RNA groove of *CUG* repeats and to alleviate RNA toxicity in myotonic dystrophy type 1 (18). To search for small molecules that can ameliorate cellular toxicity in polyQ diseases, we screened through a library of bisamidine inhibitors, and identified N^1,N^3-bis(2-(2,4,6-triaminopyrimidin-5-yl)ethyl)isophthalimidamide (Fig. 1*A*). This molecule contains one aromatic ring and two pyrimidine moieties and was originally designed for inhibiting the formation of the MBNL1-$(CCUG)^{exp}$ protein–RNA complex in myotonic dystrophy type 2 (19). We termed this compound as Anti-polyQ Aggregation for Machado-Joseph–Associated Neurodegeneration (AQAMAN). We first examined whether AQAMAN induces any detectable cytotoxicity. Up to 100 μM AQAMAN induced no detectable cell death in rat primary cortical neurons (Fig. S1*A*) and SK-N-MC cells (Fig. S1*B*).

To investigate AQAMAN's neutralizing effect on polyQ expansion–induced cytotoxicity, we utilized an established model of polyQ diseases by transfecting SK-N-MC cells with $EGFP_{CAG81(R+P)}$ (expressing both expanded *CAG* RNA and polyQ protein) (20), and we assessed the levels of cell death using an established lactate dehydrogenase (LDH) cytotoxicity assay (21). Cells expressing the pathogenic $EGFP_{CAG81(R+P)}$ displayed significantly higher levels of cell death compared with the control cells expressing $EGFP_{CAG19(R+P)}$ (Fig. 1*B*). We found that the application of 0.5 μM AQAMAN partially suppressed the $EGFP_{CAG81(R+P)}$-induced cell death (Fig. 1*B*). Increasing the concentration of AQAMAN to 1.0 or 2.0 μM had no further suppression on cell death, indicating that the suppressive effect had already reached saturation at 0.5 μM in this model (Fig. 1*B*). To determine whether AQAMAN suppressed cell death by neutralizing RNA toxicity and/or protein toxicity, we utilized an expanded *CAG* RNA toxicity model of polyQ diseases by expressing $EGFP_{CAG78(R)}$ (RNA toxicity) in SK-N-MC cells (Fig. 1*C*) (22). No suppression of cell death was detected upon the treatment of cells with up to 2.0 μM AQAMAN, indicating that AQAMAN has no effect on neutralizing expanded *CAG* repeat-induced RNA toxicity (Fig. 1*C*). To ensure that the cell death suppression effect by AQAMAN is consistent in other models of polyQ diseases, we further utilized an established cell model of MJD. In this model, SK-N-MC cells expressing truncated $MJD_{CAG78(R+P)}$ ($trMJD_{CAG78(R+P)}$) possess both *CAG* RNA toxicity and polyQ protein toxicity, and they display significantly higher amounts of cell death compared with control cells expressing the control unexpanded $trMJD_{CAG27(R+P)}$ (Fig. 1*D*) (22). Although the treatment of cells with 0.5 μM AQAMAN had no suppressive effect on this model, 1.0 and 2.0 μM AQAMAN treatment significantly suppressed cell death (Fig. 1*D*). Apart from the codon *CAG*, *CAA* also encodes for glutamine. Thus, in a construct that carries interrupted *CAA/CAG* repeats, the RNA toxicity component is disrupted while protein toxicity is retained (22, 23). Similar to cells expressing $trMJD_{CAG78(R+P)}$, cells expressing $trMJD_{CAA/G78(P)}$ (protein toxicity) exhibited an increased amount of cell death (Fig. 1*E*). Application of 0.5 μM AQAMAN in this model was sufficient to achieve a robust suppression of cell death, indicating that AQAMAN suppressed polyQ protein-induced cell death (Fig. 1*E*). Increasing the concentration of AQAMAN to 1.0 or 2.0 μM had no further effect, indicating that AQAMAN's suppression on polyQ protein toxicity was already saturated at 0.5 μM (Fig. 1*E*).

AQAMAN reduces the aggregation of polyQ proteins

To determine how AQAMAN suppresses polyQ protein-induced cell death, we transfected SK-N-MC cells with $EGFP_{CAG81(R+P)}$ and performed immunocytochemistry (ICC) to visualize polyQ aggregation with or without AQAMAN treatment. We found that 1.0 μM AQAMAN effectively reduced polyQ-containing EGFP aggregation in the $EGFP_{CAG81(R+P)}$-transfected SK-N-MC cells (Fig. 2, *A* and *B*). Consistently, 1.0 μM AQAMAN also effectively reduced polyQ-containing aggregation in SK-N-MC cells expressing EGFP-tagged $trMJD_{CAG78(R+P)}$ (Fig. 2, *C* and *D*). Importantly, similar protective effects of AQAMAN were also observed in rat cortical neurons transfected with $EGFP_{CAG81(R+P)}$ (Fig. 2, *E* and *F*) or EGFP-tagged $trMJD_{CAG78(R+P)}$ (Fig. 2, *G* and *H*), demonstrating the neuroprotective effect of AQAMAN.

In addition to ICC, filter trap and Western blotting analyses were performed to assess the effectiveness of AQAMAN in reducing polyQ protein aggregation. In our filter trap assay, we showed that 0.5 μM AQAMAN treatment resulted in a detectable reduction of EGFP–Q81 protein aggregation (Fig. 3*A*). Consistent with our results in the cell death assay shown in Fig. 1*B*, increasing the concentration of AQAMAN to 1.0 or 2.0 μM had no further anti-aggregation effect (Fig. 3*A*), indicating that saturation was reached at 0.5 μM in this model. Meanwhile, Western blot analysis showed that, upon AQAMAN treatment, soluble EGFP–Q81 level increased (Fig. 3*B*). To ensure that the

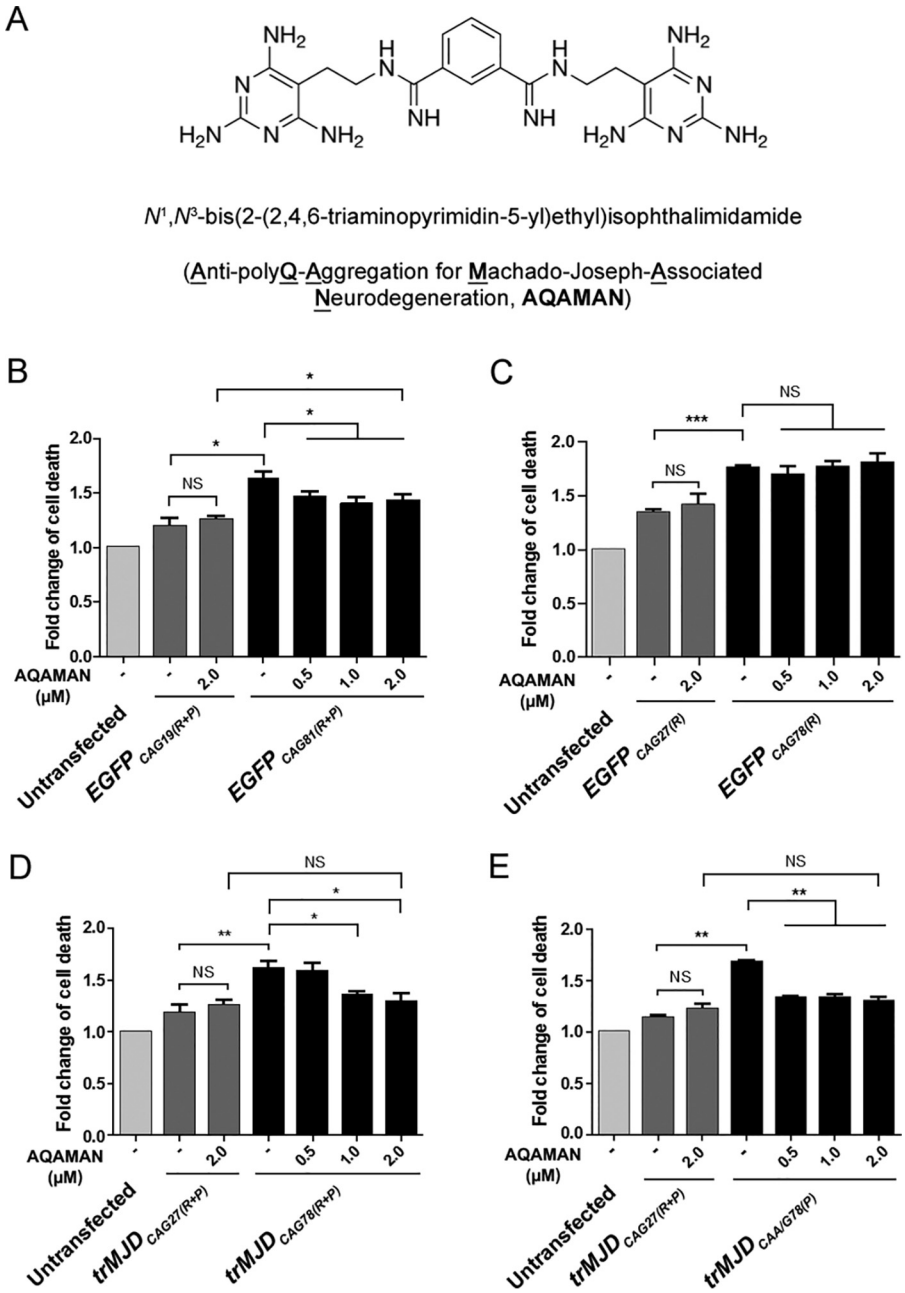

Figure 1. AQAMAN specifically neutralizes polyQ protein-mediated toxicity. *A,* chemical structure of AQAMAN. *B–E,* LDH assay using different SK-N-MC cell models of polyQ diseases. *B,* AQAMAN suppressed cell death induced by $EGFP_{CAG81}$ (*R* + *P*: RNA + protein toxicity). *C,* AQAMAN showed no suppression effect on cell death induced by $EGFP_{CAG78}$ (*R*: RNA toxicity). *D,* AQAMAN suppressed cell death induced by $trMJD_{CAG78}$ (*R* + *P*: RNA + protein toxicity). *E,* AQAMAN suppressed cell death induced by $trMJD_{CAS/G78}$ (*P*: protein toxicity). *Error bars* represent S.E. All experiments were performed at least three times independently.

increase of soluble polyQ proteins was not due to altered total protein expression, we performed formic acid treatment on the samples to solubilize the polyQ proteins (24). Our results showed that the total amount of protein remained unchanged (Fig. 3*C*). We then further tested AQAMAN's anti-aggregation effect on our MJD model of $trMJD_{CAG78(R+P)}$ expression. Consistent with our findings in the cell death assay in Fig. 1*D*, our results showed that 1.0 μM AQAMAN was sufficient to reduce trMJD–Q78 aggregation (Fig. 3*D*). In Western blot analysis, consistent with previous studies, the soluble trMJD–Q78 proteins were shown as a doublet band (25, 26). An increase in the soluble trMJD–Q78 proteins was observed when AQAMAN was applied (Fig. 3*E*). When we solubilized all proteins using formic acid, no detectable change in the total amount of protein expressed was found (Fig. 3*F*), suggesting that AQAMAN treatment increased the amount of soluble trMJD–Q78 in Fig. 3*E*.

Anti-aggregation effect of AQAMAN depends on its pyrimidine pendants

To determine whether AQAMAN prevents the formation of polyQ aggregates and/or breaks down preformed polyQ aggregates, we expressed the polyQ protein, Trx–Htt–Q46, in *Escherichia coli* and allowed the purified polyQ proteins to aggregate in a cell-free system by cleaving off the thioredoxin tag (27).

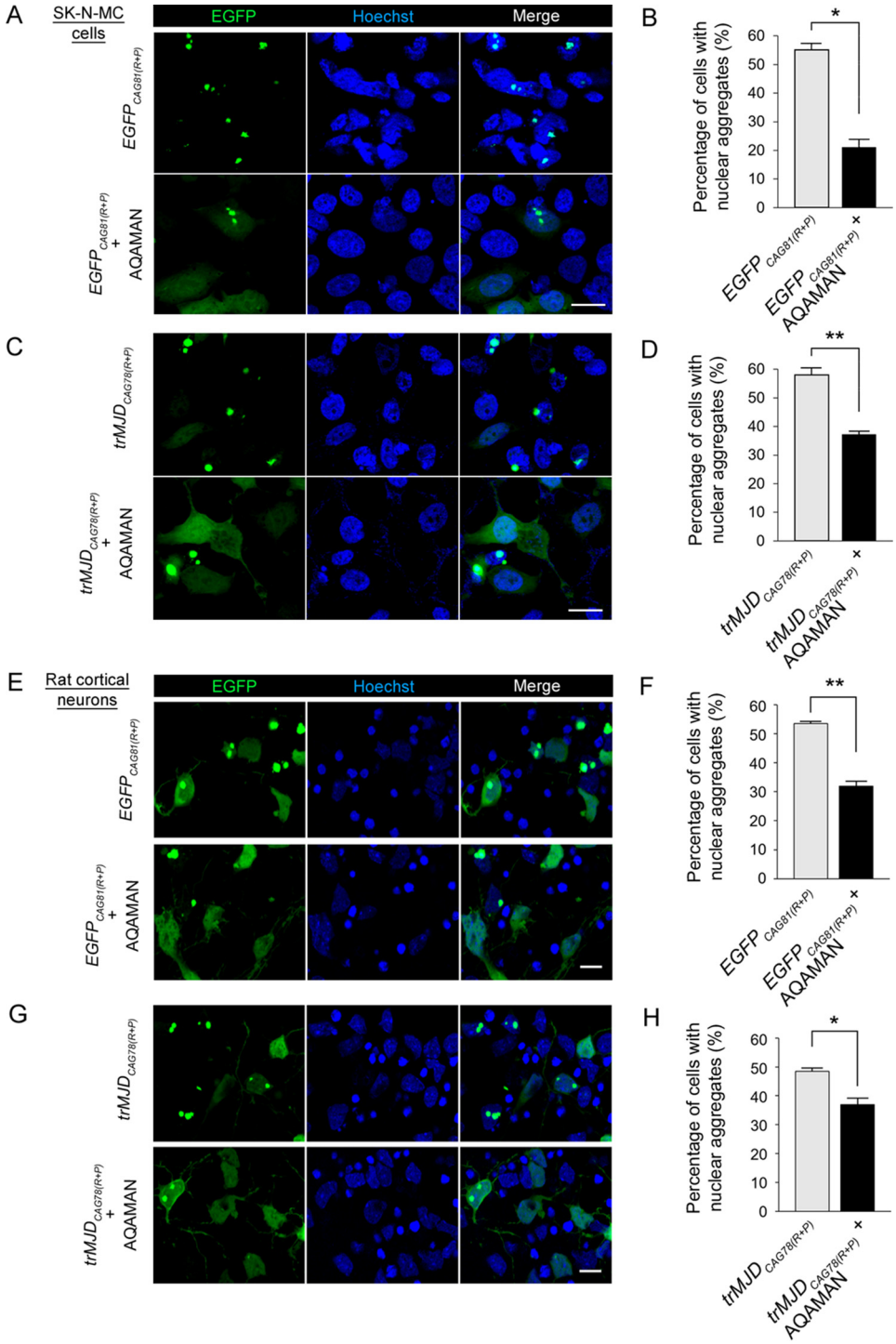

Figure 2. AQAMAN reduces nuclear aggregation of polyQ proteins. *A*, confocal micrographs of SK-N-MC cells transfected with $EGFP_{CAG81(R+P)}$. *Scale bar*, 20 μm. *B*, quantification of the percentage of cells with nuclear aggregates in *A*. *C*, confocal micrographs of SK-N-MC cells transfected with $trMJD_{CAG78(R+P)}$. *Scale bar*, 20 μm. *D*, quantification of the percentage of cells with nuclear aggregates in *C*. *E*, confocal micrographs of rat cortical neurons transfected with $EGFP_{CAG81(R+P)}$. *Scale bar*, 20 μm. *F*, quantification of the percentage of $EGFP_{CAG81(R+P)}$-expressing neurons with nuclear aggregates in *E*. *G*, confocal micrographs of rat cortical neurons transfected with $trMJD_{CAG78(R+P)}$. *Scale bar*, 20 μm. *H*, quantification of the percentage of $trMJD_{CAG78(R+P)}$-expressing neurons with nuclear aggregates in *G*. *Error bars* represent S.E. All experiments were performed at least three times independently.

We then immediately applied AQAMAN (0-h pre-aggregation) to test its ability in preventing aggregate formation. Our results showed that 50 μM AQAMAN was sufficient to significantly reduce the formation of polyQ aggregates (Fig. 4*A*), and 500 μM AQAMAN was even more effective in reducing aggregate formation (Fig. 4*A*). Thereafter, to examine whether AQAMAN can break down preformed polyQ aggregates, we applied AQAMAN after a 24-h pre-aggregation period. Our results showed that 50 μM AQAMAN was sufficient to break down the preformed aggregates *in vitro* (Fig. 4*B*), and 500 μM AQAMAN showed an even more prominent effect of breaking down preformed aggregates (Fig. 4*B*).

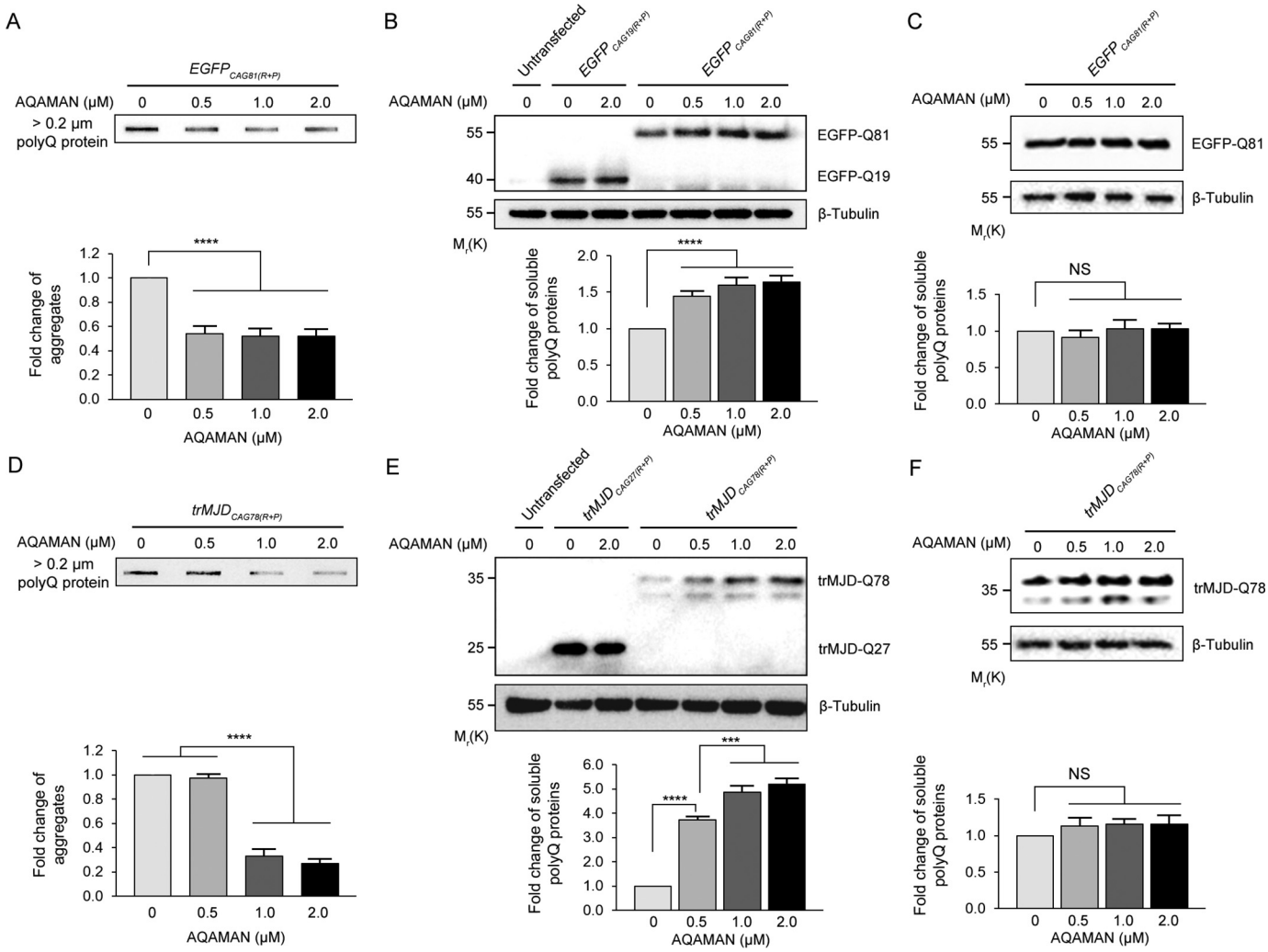

Figure 3. AQAMAN reduces polyQ aggregate levels. *A,* filter trap analysis of lysates prepared from transfected SK-N-MC cells showing reduction of aggregated polyQ-containing EGFP in response to AQAMAN. *B,* Western blot analysis on transfected SK-N-MC cells, showing the increase of soluble EGFP–Q81 proteins in response to AQAMAN. *C,* Western blot analysis on formic acid–treated samples, showing that the total EGFP–Q81 protein levels did not change in response to AQAMAN treatment. *A–C,* anti-Myc was used to detect EGFP–Q19 and EGFP–Q81, and anti-β-tubulin was used for loading controls. *D,* filter trap analysis of lysates prepared from transfected SK-N-MC cells, showing reduction of aggregated trMJD–Q78 proteins in response to AQAMAN. *E,* Western blot analysis on transfected SK-N-MC cells showing the increase of soluble trMJD–Q78 proteins in response to AQAMAN. *F,* Western blot analysis on formic acid-treated samples, showing that the total trMJD–Q78 protein levels did not change in response to AQAMAN treatment. *D–F,* anti-HA was used to detect trMJD–Q27 and trMJD–Q78, and anti-β-tubulin was used for loading controls. *Error bars* represent S.E. All experiments were performed at least three times independently.

To determine what structural features of AQAMAN contribute to its anti-aggregation effect, we synthesized another bisamidine control compound, AMD1. The general chemical features of AQAMAN and AMD1 are similar, both compounds are bisamidines with two aromatic pendants linked to the central aromatic core via a short alkyl linker, except that the pyrimidine pendants of AQAMAN were replaced by phenol units (Fig. 4*C*). AMD1 was unable to prevent the formation of polyQ aggregates (Fig. 4*D*) nor was it able to break down preformed polyQ aggregates (Fig. 4*E*). This finding suggests that the ability of AQAMAN to deaggregate polyQ proteins depends on its pyrimidine pendants.

AQAMAN mitigates neurodegeneration in a Drosophila model of MJD

To investigate whether AQAMAN can mitigate polyQ protein toxicity *in vivo*, we employed an established *Drosophila* model of MJD by expressing full-length MJD_{CAG84} ($flMJD_{CAG84}$) in the fly eye using the *gmr-GAL4* driver to induce retinal degeneration (28). Flies expressing $flMJD_{CAG84}$ showed a significant reduction of rhabdomeres per ommatidium compared with control flies that were expressing the unexpanded $flMJD_{CAG27}$ (Fig. 5, *A* and *B*). $flMJD_{CAG84}$ flies fed either 40 or 80 μM AQAMAN resulted in partial rescue of retinal degeneration (Fig. 5, *A* and *B*). Results of the filter trap and Western blot analyses demonstrated that 40 and 80 μM AQAMAN treatment effectively reduced polyQ aggregation in flies (Fig. 5, *C* and *D*). Formic acid treatment was used to verify that the total flMJD–Q84 protein level was unchanged (Fig. 5*E*). To confirm that AQAMAN has no effect on RNA toxicity *in vivo*, we examined AQAMAN's effect on a RNA toxicity-only model by expressing $DsRed_{CAG100}$ in the fly eye (23). In this transgene, the *CAG* repeat was placed at the 3′ UTR of the DsRed reporter, and thus, no polyQ protein would be produced. As expected, feeding the flies with 80 μM AQAMAN was unable to rescue the $DsRed_{CAG100}$-induced retinal degenera-

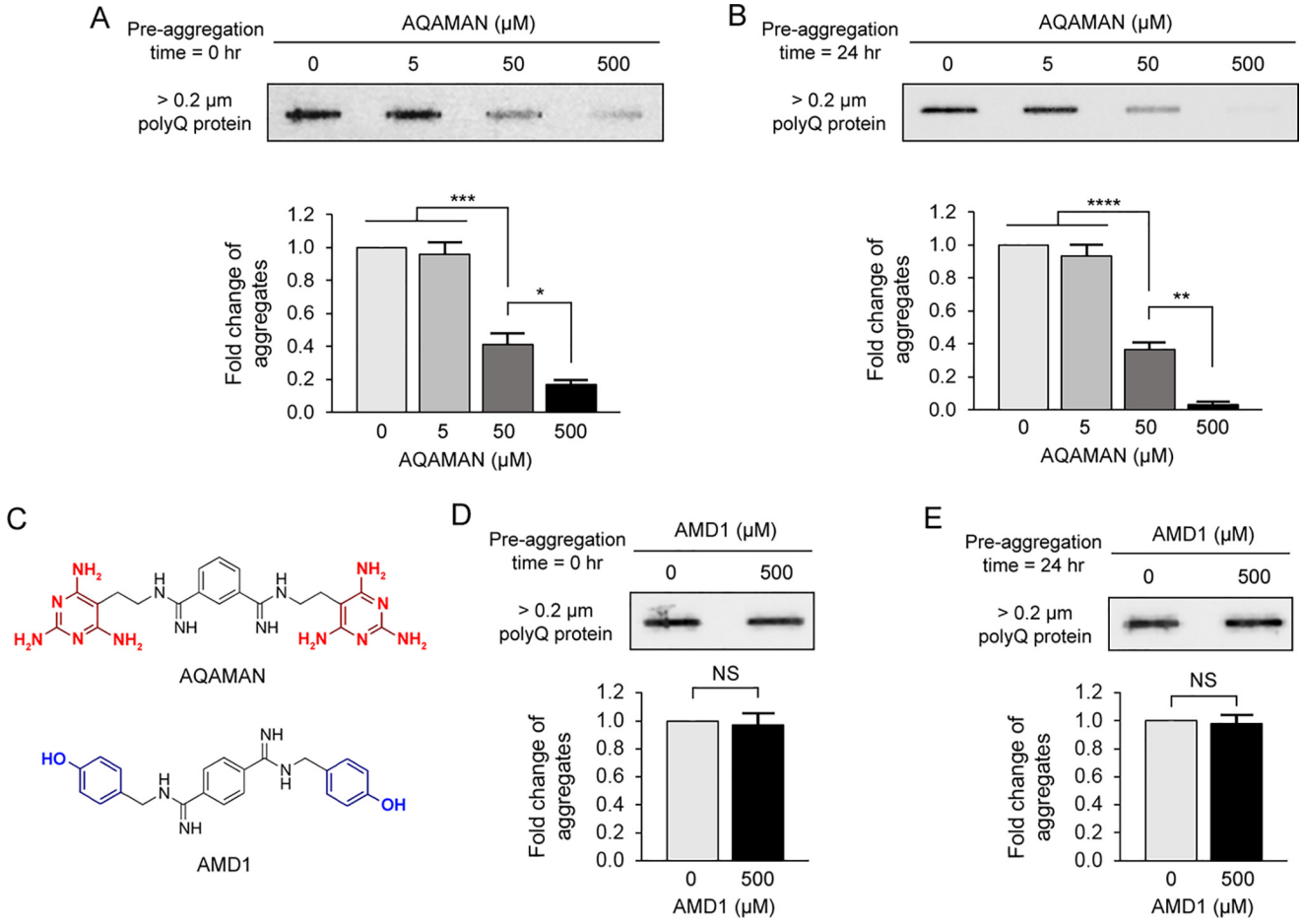

Figure 4. Anti-aggregation effect of AQAMAN depends on its pyrimidine pendants. *A,* cell-free pre-aggregation assay, showing AQAMAN's effect on polyQ protein aggregation prevention (0 h). *B,* cell-free pre-aggregation assay, showing AQAMAN's effect on deaggregation of preformed inclusions (24 h). *C,* molecular structure of AQAMAN and AMD1. AMD1 has a similar structure to AQAMAN but with the pyrimidines (*red*) replaced by phenols (*blue*). *D* and *E,* cell-free pre-aggregation assay, showing that AMD1 has no effect on polyQ protein aggregation prevention (0 h) (*D*) or deaggregation of preformed inclusions (24 h) (*E*). *Error bars* represent S.E. All experiments were performed at least three times independently.

tion caused by the RNA toxicity of the untranslated *CAG* repeats (Fig. 5, *F* and *G*). These results demonstrated that AQAMAN can ameliorate neurodegeneration *in vivo* by reducing the aggregation of polyQ proteins.

Neutralization of polyQ protein toxicity by AQAMAN requires autophagy

Autophagy is a tightly-regulated catabolic mechanism for lysosomal degradation of misfolded proteins (29). Impaired autophagy results in the accumulation of misfolded proteins, contributing to ER stress (13, 14). Even though AQAMAN is capable of reducing the aggregation of polyQ proteins, we speculated that autophagy would remain necessary for their clearance to reduce toxicity. To address this, we either blocked or induced autophagy in our cell model of polyQ diseases and examined AQAMAN's effect on cell death using LDH assay and polyQ aggregation. Wortmannin is a phosphatidylinositol 3-kinase inhibitor that impedes autophagosome formation, thereby blocking autophagy (30), whereas rapamycin is a mammalian target of rapamycin (mTOR) inhibitor that mimics cellular starvation by blocking signals required for cell growth and proliferation, which in turn activates autophagy (30). We found that blocking autophagy with wortmannin had no effect on the untransfected or the control unexpanded $trMJD_{CAG27(R+P)}$-expressing cells but resulted in increased cell death in expanded polyQ $trMJD_{CAG78(R+P)}$– expressing cells (Fig. 6*A*). Consistent with our findings in Fig. 1*D*, AQAMAN treatment suppressed cell death in $trMJD_{CAG78(R+P)}$-expressing cells (Fig. 6*A*). However, under the effect of wortmannin, AQAMAN was unable to suppress cell death in $trMJD_{CAG78(R+P)}$-expressing cells (Fig. 6*A*). These results suggested that the suppression of polyQ-induced cell death by AQAMAN depends on the autophagic pathway.

It is possible that wortmannin blocked AQAMAN's cytoprotective effect by impeding its anti-aggregation function. Thus, we performed ICC to examine polyQ aggregation under the effect of these compounds. Consistent with our findings in Fig. 2, *C* and *D*, AQAMAN treatment reduced polyQ aggregates in $trMJD_{CAG78(R+P)}$-expressing cells (Fig. 6, *B* and *C*). However, the presence of wortmannin did not prevent AQAMAN from reducing polyQ aggregates (Fig. 6, *B* and *C*). These results suggest that although the suppression of polyQ-induced cell death by AQAMAN depends on autophagy, the anti-aggregation effect of AQAMAN is independent of autophagy.

Because blocking autophagy abolished AQAMAN's effect on suppressing cell death, we sought to determine whether the

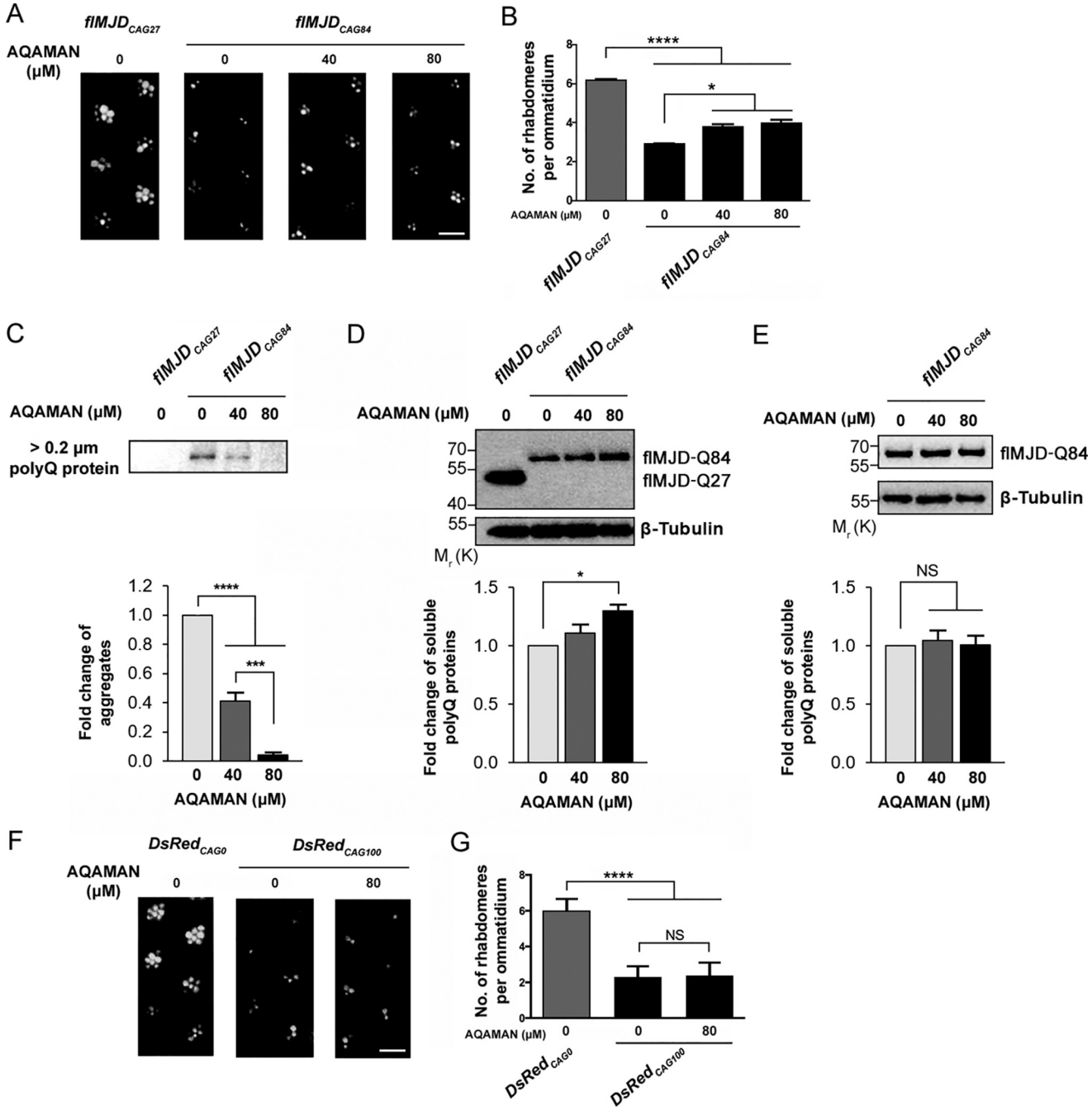

Figure 5. AQAMAN mitigates polyQ protein-induced neurodegeneration in *Drosophila*. *A,* AQAMAN partially rescued *flMJD*$_{CAG84}$-induced retinal degeneration in *Drosophila*. *Scale bar,* 50 μm. *B,* quantification of *A*. *C,* filter trap analysis of lysates prepared from fly heads, showing the reduction of flMJD–Q84 aggregates in response to AQAMAN. *D,* Western blot analysis showing the increase of soluble flMJD–Q84 proteins in response to AQAMAN. *E,* Western blot analysis on formic acid–treated samples, showing that the total flMJD–Q84 protein levels did not change in response to AQAMAN treatment. *C–E*, anti-Myc was used to detect flMJD–Q27 and flMJD–Q84, and anti-β-tubulin was used for loading controls. *F,* AQAMAN had no effect on the untranslated *DsRed*$_{CAG100}$ RNA toxicity-induced neurodegeneration. *Scale bar,* 50 μm. *G,* quantification of *F*. *Error bars* represent S.E. All experiments were performed at least three times independently.

activation of autophagy using rapamycin would enhance the cytoprotective effects of AQAMAN. Similar to the AQAMAN treatment, rapamycin treatment suppressed polyQ-induced cell death (Fig. 6*D*). When rapamycin was added to AQAMAN-treated cells, it resulted in further suppression of cell death compared with cells treated with AQAMAN alone (Fig. 6*D*), indicating that activation of autophagy could indeed further potentiate the suppressive effect of AQAMAN on polyQ-induced cell death. As for polyQ aggregation, both AQAMAN and rapamycin were capable of individually reducing cellular aggregates (Fig. 6, *E* and *F*). Application of both compounds together resulted in a further reduction of aggregates (Fig. 6, *E* and *F*). The combinatorial effect of the two compounds appeared to be additive.

AQAMAN relieves ER stress

In polyQ diseases, misfolded proteins with polyQ tracts accumulate in the ER and cause ER stress (4, 5, 7). We examined

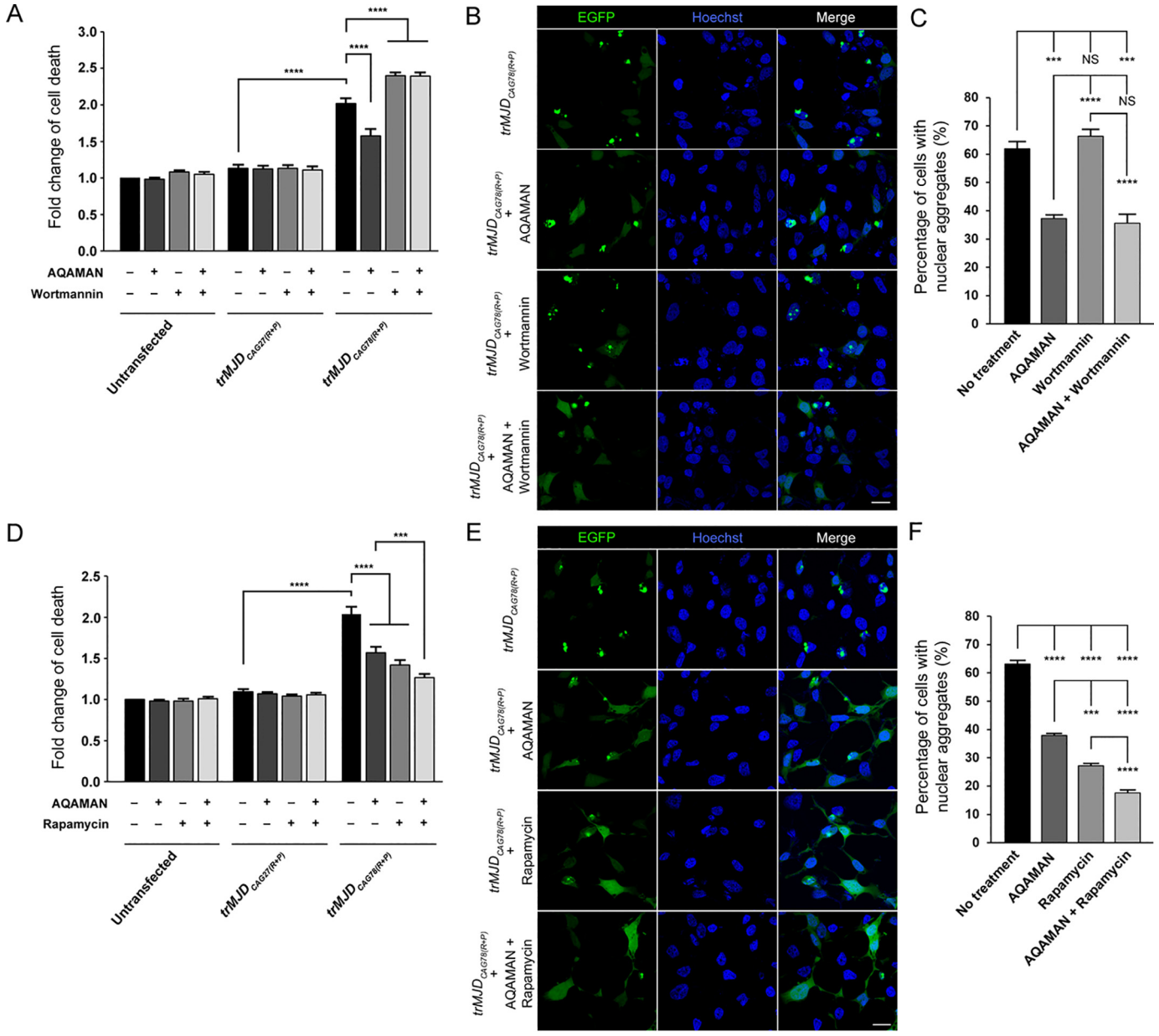

Figure 6. Suppression of polyQ-induced cell death by AQAMAN requires autophagy. *A*, LDH assay on SK-N-MC cells showing wortmannin blocking the suppression of cell death by AQAMAN. *B*, confocal micrographs of SK-N-MC cells showing AQAMAN retaining its ability to reduce polyQ aggregation under the presence of wortmannin. *C*, quantification of the percentage of cells with nuclear aggregates in *B*. *D*, LDH assay on SK-N-MC cells showing that rapamycin further increases the suppression of cell death by AQAMAN. *E*, confocal micrographs of SK-N-MC cells showing the combinatorial effect of rapamycin and AQAMAN in reducing polyQ aggregates. *F*, quantification of the percentage of cells with nuclear aggregates in *E*. *Error bars* represent S.E. All experiments were performed at least three times independently.

the transcript level of the ER stress sensor binding immunoglobulin protein (BiP). BiP is a molecular chaperone located in the ER lumen that regulates the translocation of proteins. The expression of *BiP* is up-regulated during ER stress, triggering the UPR pathway (31, 32). It has been shown that *BiP* expression is induced in polyQ diseases (33). Using quantitative RT-PCR, we demonstrated that $trMJD_{CAG78(R+P)}$-expressing SK-N-MC cells have increased expression of *BiP* compared with the control $trMJD_{CAG27(R+P)}$-expressing cells (Fig. 7*A*). We found that 0.5–2.0 μM AQAMAN effectively suppressed *BiP* induction in $trMJD_{CAG78(R+P)}$-expressing cells (Fig. 7*A*), suggesting that ER stress was relieved. To further investigate whether similar effects could be observed *in vivo*, we examined whether AQAMAN treatment could reduce *BiP* transcript levels in the $flMJD_{CAG84}$ *Drosophila* model. Consistently, 40 and 80 μM AQAMAN restored *BiP* transcription level back to that of control (Fig. 7*B*). These results demonstrated that AQAMAN could relieve polyQ-induced ER stress *in vitro* and *in vivo*.

Discussion

The abnormal aggregation of proteins is a hallmark of many neurodegenerative diseases, such as Alzheimer's disease, Parkinson's disease, and polyQ diseases (34). Because mutant protein aggregates have been shown to exhibit cellular toxicity (35) and even have the potential to spread to

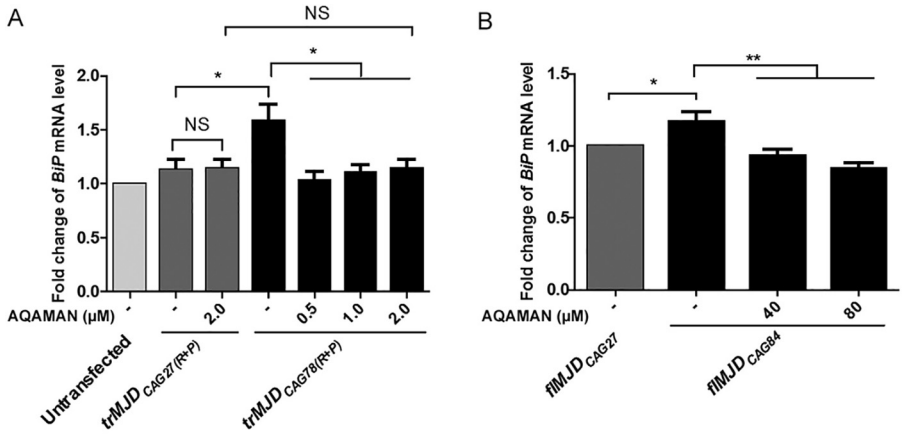

Figure 7. AQAMAN ameliorates ER stress. *A,* quantitative RT-PCR showing AQAMAN restoring normal *BiP* mRNA level in a SK-N-MC cell model of MJD. *B,* quantitative RT-PCR showing AQAMAN restoring normal *BiP* mRNA level in a *Drosophila* model of MJD. *Error bars* represent S.E. All experiments were performed at least three times independently.

other cells and brain regions (36), controlling protein aggregation is therefore paramount to combating these neurodegenerative diseases.

Polyglutamine aggregates are mainly composed of fibers with β-sheet structure, which is similar to amyloid in Alzheimer's disease (3, 37, 38). In this study, we identified AQAMAN as a novel anti-polyQ aggregation compound. We showed that AQAMAN is capable of suppressing cell death (Fig. 1, *B–E*) and neurodegeneration (Fig. 5) induced by polyQ protein toxicity. Moreover, we demonstrated that AQAMAN can prevent polyQ aggregation and dissociate preformed polyQ aggregates *in vitro* (Fig. 4), which suggests that AQAMAN can likely bind to the soluble forms of the polyQ proteins and shift the aggregation equilibrium toward the soluble forms of the proteins. This effect was absent with the structurally similar AMD1, indicating that this binding was likely via the two pyrimidine pendants of AQAMAN (Fig. 4).

Two major pathways are responsible for degrading misfolded proteins in the cell: the ubiquitin–proteasome pathway and the autophagy pathway (29). When proteins are accessible to both pathways, the ubiquitin–proteasome system is the prioritized clearance route due to its higher efficiency. However, if a protein is aggregate-prone and the proteasomes fail to degrade the protein aggregates, then the autophagy pathway will become the main clearance route (29). Autophagy was originally identified as a self-consuming cellular process and was later found to be involved in the degradation of misfolded proteins as a cytoprotective response especially during aging and neurodegeneration (39). The autophagy pathway plays a pivotal role in the degradation of polyQ proteins and protects the cell from polyQ-induced neurodegeneration and cell death (40, 41). Despite the fact that AQAMAN can deaggregate polyQ proteins (Figs. 3 and 4), it is possible that the deaggregated polyQ proteins still exhibit substantial cytotoxicity and require clearance by the autophagy pathway. In fact, it was reported that large protein aggregates may not be toxic and that the smaller microaggregates may be the actual major toxic species (42, 43). Indeed, recent studies have revealed that even deaggregated polyQ proteins may also be toxic (44). This is consistent with our observation that blocking autophagy does not affect AQAMAN's ability to reduce polyQ aggregation (Fig. 6, *B* and *C*) but abolished its effect on suppressing cell death (Fig. 6*A*). These results suggest that the dissociation of insoluble aggregates does not prevent cell death. Even after AQAMAN has broken down the visible aggregates, there may still be toxic species in the cell, such as microaggregates or soluble small oligomers that can contribute to polyQ-induced cytotoxicity. Functional autophagic pathways are still required for the proper clearance of these toxic species.

Previous studies have shown that the autophagy activator rapamycin can protect against polyQ-induced toxicity (45), and its cytoprotective effect depends on the activation of autophagy for the clearance of polyQ proteins (46, 47). In line with these studies, we demonstrated that increasing the level of autophagy with rapamycin results in further reduction of polyQ aggregate and cell death in AQAMAN-treated cells (Fig. 6, *D–F*).

The accumulation of unfolded/misfolded polyQ proteins causes ER stress (4, 5, 7). Clearance of unfolded/misfolded proteins in the ER primarily relies on the UPR pathway, which induces the expression of molecular chaperones and folding enzymes for the ER to cope with the deleterious effects of unfolded/misfolded proteins (10, 11). Our results showed that AQAMAN ameliorates polyQ-induced ER stress (Fig. 7). It is possible that the level of polyQ proteins deaggregated by AQAMAN are being kept low in the cell by autophagy. This, in turn, reduces the accumulation of unfolded/misfolded polyQ proteins in the ER, thereby relieving ER stress.

To further examine polyQ deaggregation by AQAMAN, we performed isothermal titration calorimetry (ITC) to study whether AQAMAN binds to Trx–Htt–Q46. Preliminary ITC results indicate a weak interaction between AQAMAN and Trx–Htt–Q46 (Fig. S2), suggesting that AQAMAN may not bind to the protein monomer, but its ability to reduce polyQ aggregation may be due to its binding to other soluble forms of the protein. More importantly, the observations that AQAMAN can both prevent the formation and solubilize the insoluble polyQ aggregates (Fig. 4, *A* and *B*) suggest that the polyQ aggregation and precipitation equilibria are reversible with no obvious kinetic effect. The ability of AQAMAN to sol-

ubilize polyQ aggregates could therefore be attributed to its ability to bind to the soluble forms of the protein, which shifts the aggregation equilibrium from the insoluble aggregate to the soluble forms. This binding of AQAMAN to soluble polyQ proteins depends on the two pyrimidine pendants in its chemical structure as we showed that AMD1 did not have this effect (Fig. 4, *D* and *E*). Given the complexity of the polyQ aggregation equilibria involving different soluble forms of the protein and the insoluble aggregates, more elaborated binding studies on de-convoluting the heat profile to individual equilibrium will be necessary for a more detailed mechanistic insight. Nevertheless, it is clear that AQAMAN can inhibit the formation of the polyQ aggregates and neutralize its toxicity.

Many potential therapeutics against polyQ diseases have been previously reported. These therapeutics include but are not limited to small molecules and peptide inhibitors. Calmidazolium chloride was previously reported to prevent expanded polyQ-containing Huntingtin exon1 (Httex1) from aggregating (48). However, unlike AQAMAN, calmidazolium chloride targets only the initial step of Httex1 aggregation. Other polyQ small molecule inhibitors include those that modulate insulin/insulin-like growth factor signaling (49), inhibit the Rho-associated kinase (50), Hsp90 (51), and topoisomerase 1 (52) or accelerate autophagy (53, 54). Peptide inhibitors, such as QBP1 (55), can inhibit polyQ aggregation by impeding the β-sheet conformational transition of the polyQ protein monomer as well as oligomer formation (56, 57), whereas other peptide inhibitors, such as P3, P3V8, and TAT-BIND, that can bind directly to *CAG* RNA suppress RNA toxicity (58–60). Although these peptide-based drugs are effective in reducing polyQ-induced cytotoxicity, their large molecular size may hinder them from crossing the blood–brain barrier (BBB). By contrast, small molecules are likely to be more efficient in penetrating the BBB. To assess whether AQAMAN can penetrate the BBB, we employed the on-line Blood Brain Barrier Predictor developed by Xie and co-workers (61). AQAMAN is indeed predicted to be able to penetrate the BBB (Fig. S3).

In this study, we identified AQAMAN as a small molecule that can ameliorate polyQ-induced protein toxicity by deaggregating polyQ inclusions. However, one apparent limitation of AQAMAN is its risk in promoting the buildup of small toxic oligomers or microaggregates and its dependence on functional autophagic pathways to properly relieve the cell from polyQ toxicity. AQAMAN treatment under impaired autophagy may accelerate the accumulation of such toxic species and may actually be harmful to the cell. Nevertheless, AQAMAN is a potent polyQ aggregation inhibitor that can likely cross the BBB, and thus, it has great therapeutic potential in bringing relief to patients suffering from incurable protein aggregation diseases.

Summary

We demonstrated the effect of AQAMAN in alleviating protein toxicity in several models of polyQ diseases. *In vitro*, AQAMAN can deaggregate polyQ proteins and suppress cell death in an autophagic pathway-dependent manner, whereas *in vivo*, AQAMAN can relieve polyQ-induced ER stress and ameliorate neurodegeneration. These results underpin the potentials of AQAMAN as a therapeutic for polyQ diseases. Our study also highlights the importance of the autophagy pathway in the clearance of deaggregated polyQ proteins.

Experimental procedures

DNA constructs and recombinant protein

The DNA constructs *pcDNA3.1-Q19-EGFP-myc*, *pcDNA3.1-Q81-EGFP-myc* (used in Figs. 1*B* and 2*A*); *pEGFP-C1-EGFP*$_{CAG27}$ and *pEGFP-C1-EGFP*$_{CAG78}$ (used in Fig. 1*C*); *pcDNA3.1*(+)-*HA-trMJD*$_{CAG27}$, *pcDNA3.1*(+)-*HA-trMJD*$_{CAG78}$, and *pcDNA3.1*(+)-*HA-trMJD*$_{CAA/G78}$*D* (used in Fig. 1*D*) were previously reported (20, 22, 62). To generate the *pEGFP-trMJD*$_{CAG27}$ and *pEGFP-trMJD*$_{CAG78}$ (used in Fig. 2*C*), the *trMJD*$_{CAG27}$ and *trMJD*$_{CAG78}$;DNA sequences were amplified from *pcDNA3.1*(+)-*HA-trMJD*$_{CAG27}$ and *pcDNA3.1*(+)-*HA-trMJD*$_{CAG78}$ using primers *EGFP-MJD-polyQ-F*, 5′-CCGGGTACCCCGCTTCGGAAGAGACGAG-3′ and *EGFP-MJD-polyQ-R*, 5′-CCGGGATCCCGGCCGCAGATCTGCTC-3′. The resulting DNA fragments were subcloned into *pEGFP-C1* vector (Addgene, Cambridge, MA) using KpnI and BamHI. Constructs *pET32a-Trx–Htt–Q46* and *pET32a-Trx* were obtained from Addgene, Cambridge, MA. The Trx and Trx–Htt–Q46 proteins were induced, expressed, and purified according to a published method (27). Purified proteins were stored at 50 mM Tris-HCl, pH 8.0, 150 mM NaCl, 1 mM PMSF, and 1 mM EDTA at −80 °C.

Chemicals

AQAMAN was prepared from diethyl isophthalimidate dihydrochloride (16) and characterized using ^{1}H nuclear magnetic resonance (NMR) and LC-MS. The ^{1}H NMR spectra were obtained using a Brucker DPX 400 spectrometer. Signals were internally referenced to solvent residues of DMSO-d_6 at 2.50 ppm. ^{1}H NMR (DMSO, 298 K) δ 2.79 (4H, t, J = 7.38 Hz), 3.57 (4H, t, J = 7.08 Hz), 6.86 (4H, s), 7.07 (8H, s), 7.87 (1H, t, J = 7.60 Hz), 8.16 (2H, d, J = 9.18 Hz), 8.50 (1H, s), 9.62 (2H, s), 9.84 (2H, s), 10.34 (2H, s). LC-MS was performed using a Waters-Alliance e2695 system coupled to a 2489 UV-visible detector and an ACQUITY QDa MS detector. HPLC analysis was carried out using a SunFire^{TM} C8 column (4.6 × 250 mm, 5-μm particle size) using a gradient elution (Fig. S4). Electrospray ionization–mass spectrometer (ESI-MS) (+ve) for AQAMAN: m/z = 465.3 $[M + H]^+$, 233.1 $[M + 2H]^{2+}$; M = free base of AQAMAN. The AQAMAN was dissolved with autoclaved ddH_2O and stocked as 10 mM. AMD1 was synthesized by stirring a suspension of diethyl terephthalimidate dihydrochloride (0.24 g, 0.81 mmol) in 30 ml of dry ethanol with 4-hydroxylbenzylamine (0.25 g, 2.0 mmol) and triethylamine (0.34 ml, 2.4 mmol) at room temperature overnight. The white precipitate formed was collected by vacuum filtration and washed with ethanol and diethyl ether. The white solid was resuspended in 15 ml of saturated ethanolic hydrogen chloride solution and stirred at 60 °C for 4 h. The mixture was cooled to room temperature, and the resulting white precipitate was collected by vacuum filtration and washed with ethanol and diethyl ether. Yield was 0.27 g, 74%. ^{1}H NMR (500 MHz, DMSO-d_6, 298 K): δ 9.89 (br s, 2 H), 9.66 (br s, 4 H), 7.99 (s, 4 H), 7.31 (d, J = 10.0, 4

H), 6.80 (d, $J = 10.0$, 4 H), 4.61 (s, 4 H), and $^{13}C\{^{1}H\}$ NMR (125 MHz, DMSO-d_6, 298 K): δ 161.5, 157.3, 132.9, 129.4, 128.8, 125.5, 115.4, 45.5. ESI-MS (+ve) found 375.3 $[M + H]^+$. Wortmannin (Sigma) and rapamycin (Santa Cruz Biotechnology, Inc., Dallas, TX) were both dissolved in DMSO. Wortmannin was used at 1 μM, and the treatment lasted for 72 h. Rapamycin was used at 2 μM, and the treatment lasted for 6 h.

Drosophila culture and drug treatment

The *Drosophila* strains *UAS-flMJD*$_{CAG27}$, *UAS-flMJD*$_{CAG84}$ (28), *UAS-DsRed*$_{CAG0}$, and *UAS-DsRed*$_{CAG100}$ (23) used in this study were from Professor Nancy Bonini (University of Pennsylvania). *gmr-GAL4* was obtained from Bloomington *Drosophila* Stock Center. *Drosophila* strains were cultured with cornmeal yeast glucose agar medium and maintained at 22 °C. Genetic crosses were also carried out at 22 °C. AQAMAN solution was added into fresh medium, which was subsequently used for fly culture.

Drosophila pseudopupil assay

Details of the assay were previously described (6). In a typical procedure, fly heads were cut and observed under light microscopy (Olympus BX51, Tokyo, Japan) with a ×60 oil objective. Images of ommatidia were captured using the SPOT Advanced software (Version 4.1; Diagnostic Instruments Inc., Sterling Heights, MI). For quantification of ommatidia integrity, a total of 200 ommatidia from 20 eyes of 10 individual flies were examined in each condition. The average number of rhabdomeres per ommatidium was counted. Each experiment was repeated at least three times.

SK-N-MC cell culture and drug treatment

The human neuroblastoma cell line SK-N-MC cells were obtained from ATCC (Manassas, VA) and cultured using DMEM (Hyclone; ThermoFisher Scientific, Waltham, MA) supplemented with 4 mM L-glutamine, 10% fetal bovine serum, and 1% penicillin-streptomycin. The cells were maintained at 37 °C under 95% air, 5% CO_2. For cells subjected to LDH assays, phenol red-free DMEM (Life Technologies, Inc., and ThermoFisher Scientific, Waltham, MA) was used for culturing. The AQAMAN solution was added into the medium at the same time of transfection and the treatment lasted for 72 h.

Primary rat cortical neurons

The primary rat cortical neurons were prepared as described previously (6). In brief, the cells were isolated from E18 rat embryos and cultured at 24-well plates pre-coated with poly-D-lysine (Sigma). Neurons were maintained in Neurobasal Medium (Invitrogen; ThermoFisher Scientific) supplied with 2% B-27 (Invitrogen; ThermoFisher Scientific), 1% penicillin/streptomycin (ThermoFisher Scientific), and 2 mM glutamine (Invitrogen; ThermoFisher Scientific).

Transfection conditions

For the transfection of SK-N-MC cells, the cells were seeded at a density of 0.8×10^5 cells/24-well plate. After 24 h, 1 μg of plasmid DNA was used to transfect cells using Lipofectamine 2000 reagent (Invitrogen; ThermoFisher Scientific). For the transfection of primary rat cortical neurons, the neurons were incubated with 3 μg of plasmids in primary neuron transfection reagent (VVPG-1003, Lonza Bioscience), followed by transfection using Amaxa Nucleofection system (Lonza Bioscience) according to the manufacturer's instructions.

Lactate dehydrogenase cytotoxicity assay

Details of the assay were previously described (21, 60). CytoTox 96® nonradioactive cytotoxicity assay kit (Promega, Madison, WI) was used to study cell viability. Both of the LDH released from culture medium and adherent cells were obtained, representing dead and survival cells, respectively. The percentage of cell death was calculated and normalized to the untransfected control.

Immunofluorescence staining

SK-N-MC cells were seeded on coverslips in 24-well plates. The culture medium was discarded, and cells were fixed with 3.7% formaldehyde fixative solution and permeabilized with 0.1% Triton X-100. After blocking with 5% goat serum, the cell nuclei were stained with 5 μM Hoechst 33342 solution (Invitrogen; ThermoFisher Scientific). For the immunostaining performed on primary rat cortical neurons, the neurons were cultured at 12-well plates with coverslips and pre-coated with poly-D-lysine (Sigma). Confocal microscopy was performed on Leica TCS SP8 with software control of LAS X (Leica Microsystems CMS GmbH, Mannheim, Germany). Image analysis was performed using ImageJ (National Institutes of Health, Bethesda, MD) and Adobe Photoshop 7.0 software (Adobe, San Jose, CA). For quantification analysis, the percentage of cells that contain aggregated protein in transfected cells was calculated. For each group, over 200 cells were counted.

Quantitative real-time PCR (qRT-PCR)

A total of 10 adult fly heads or cultured cell samples (in standard 24-well plates) were homogenized in TRIzol reagent for extracting RNA. One microgram of RNA was then subjected to reverse transcription using the ImPromII™ reverse transcription system (Promega, Madison, WI). TaqMan® probe qRT-PCR was applied to detect mRNA expression level. Quantification of target gene expression level was calculated using the $2^{-\Delta\Delta Ct}$ method. The TaqMan® probes (ThermoFisher Scientific) used in this study are as follows: human *BiP* (Hs99999174_m1); human β-actin (*ACTB*) (Hs99999903_m1); *Drosophila BiP* (Dm01813415_g1); and *Drosophila GADPH* (Dm01841186_g1).

Western blot analysis

Ten adult fly heads or cultured SK-N-MC cell samples (in standard 24-well plates) were homogenized/lysed with 2% SDS buffer with a plastic pestle for protein extraction. Protein concentration was detected using the Pierce™ bicinchoninic acid protein assay kit (ThermoFisher Scientific). Primary antibodies used in Western blot analyses are listed as follows: HA-7 (Sigma; 1:1,000) for the detection of HA-tag; 9B11 (Cell Signaling Technology, Inc., Danvers, MA; 1:1,000) for Myc-tag; and Ab6046 (Abcam, Cambridge, UK; 1:2,000) for

β-tubulin. The protein chemiluminescence signal was obtained and visualized with the ChemiDoc™ Touch Gel Imaging System (Bio-Rad). The images were analyzed with ImageLab™ software (Bio-Rad).

Recombinant protein aggregates formation

The recombinant protein aggregate formation in a cell-free condition was previously described (63). In a typical procedure, aggregation was initiated by adding enterokinase (EK) (Ipswich, MA) into 10 μM purified recombinant Trx–Htt–Q46 protein to cleavage the Trx tag from polyQ protein. AQAMAN was added at the time of adding EK (to inhibit formation of aggregates) or after 24 h of adding EK (to dissociate preformed aggregates). The mixture was then incubated at 30 °C for 72 h to form the aggregates or to dissociate the preformed aggregates. To stop the reaction, an equal volume of 4% SDS was added to each sample, followed by boiling at 99 °C for 10 min. The presence of aggregates was detected using a filter trap assay.

Filter trap assay

SK-N-MC cells cultured in standard 24-well plates were lysed in 2% SDS solution and collected. Protein samples were diluted to a final volume of 200 μl with the same solution. The protein sample was then transferred to 48-well Bio-Dot® microfiltration apparatus and filtered with cellulose acetate membrane (pore size 0.2 μm; Sartorius Stedim Biotech Gmbh, Goettingen, Germany). The membrane was blocked with 5% nonfat dry milk and incubated with antibodies (same antibodies used for Western blottings) for aggregated protein detection.

ITC

ITC-binding assay was performed on MicroCal iTC 200 (Malvern Instruments Ltd., Malvern, UK). AQAMAN was dissolved in autoclaved ddH_2O and diluted to 6 mM with protein buffer (50 mM Tris, 150 mM NaCl, 1 mM PMSF, 1 mM EDTA, pH 8.0). With the system temperature set at 25 °C, 6 mM AQAMAN was titrated against 0.2 mM of Trx protein or Trx–Htt–Q46 protein. Titration results were analyzed with Origin® scientific plotting software version 7 (OriginLab Corp.) and fitted with sequential binding sites model.

Statistical analysis

For comparisons between three or more sample groups, analysis of variance with the Tukey post hoc test was performed. For pairwise comparisons, a Student's *t* test was used. *, $p < 0.05$; **, $p < 0.01$; ***, $p < 0.001$. NS indicates not significant. All histograms depict mean ± S.E. All experiments were performed at least three times independently.

Institutional animal care and use

The animal research in this study was approved by the Animal Experimentation Ethics Committee of the Chinese University of Hong Kong.

Author contributions—H. H., A. C. K., Z. S. C., K.-F. L., J. C. K. N., H. Y. A.-Y., and H. Y. E. C. conceptualization; H. H., A. C. K., Z. S. C., K.-F. L, J. C. K. N., C.-H. W., H. Y. A.-Y., S. C. Z., and H. Y. E. C. data curation; H. H. and Z. S. C. formal analysis; H. H., A. C. K., H. Y. A.-Y., and H. Y. E. C. validation; H. H., A. C. K., Z. S. C., Y. W., Y. A., W. L., and M. H. Y. L. investigation; H. H., A. C. K., Z. S. C., K.-F. L., J. C. K. N., H. Y. A.-Y., S. C. Z., and H. Y. E. C. methodology; H. H., A. C. K., and Z. S. C. writing-original draft; H. H., A. C. K., and H. Y. E. C. project administration; H. H., A. C. K., H. Y. A.-Y., S. C. Z., and H. Y. E. C. writing-review and editing; A. C. K., K.-F. L., J. C. K. N., H. Y. A.-Y., and H. Y. E. C. supervision; S. C. Z. and H. Y. E. C. resources; M. H. Y. L., H. Y. A.-Y., S. C. Z., and H. Y. E. C. funding acquisition; H. Y. E. C. software.

References

1. Zoghbi, H. Y., and Orr, H. T. (2000) Glutamine repeats and neurodegeneration. *Annu. Rev. Neurosci.* **23,** 217–247 CrossRef Medline
2. Orr, H. T., and Zoghbi, H. Y. (2007) Trinucleotide repeat disorders. *Annu. Rev. Neurosci.* **30,** 575–621 CrossRef Medline
3. Ross, C. A. (2002) Polyglutamine pathogenesis: emergence of unifying mechanisms for Huntington's disease and related disorders. *Neuron* **35,** 819–822 CrossRef Medline
4. Kouroku, Y., Fujita, E., Jimbo, A., Kikuchi, T., Yamagata, T., Momoi, M. Y., Kominami, E., Kuida, K., Sakamaki, K., Yonehara, S., and Momoi, T. (2002) Polyglutamine aggregates stimulate ER stress signals and caspase-12 activation. *Hum. Mol. Genet.* **11,** 1505–1515 CrossRef Medline
5. Duennwald, M. L., and Lindquist, S. (2008) Impaired ERAD and ER stress are early and specific events in polyglutamine toxicity. *Genes Dev.* **22,** 3308–3319 CrossRef Medline
6. Chen, Z. S., Li, L., Peng, S., Chen, F. M., Zhang, Q., An, Y., Lin, X., Li, W., Koon, A. C., Chan, T. F., Lau, K. F., Ngo, J. C. K., Wong, W. T., Kwan, K. M., and Chan, H. Y. E. (2018) Planar cell polarity gene Fuz triggers apoptosis in neurodegenerative disease models. *EMBO Rep.* **19,** e45409 CrossRef Medline
7. Jiang, Y., Chadwick, S. R., and Lajoie, P. (2016) Endoplasmic reticulum stress: the cause and solution to Huntington's disease? *Brain Res.* **1648,** 650–657 CrossRef Medline
8. Rusmini, P., Crippa, V., Cristofani, R., Rinaldi, C., Cicardi, M. E., Galbiati, M., Carra, S., Malik, B., Greensmith, L., and Poletti, A. (2016) The role of the protein quality control system in SBMA. *J. Mol. Neurosci.* **58,** 348–364 CrossRef Medline
9. Fardghassemi, Y., Tauffenberger, A., Gosselin, S., and Parker, J. A. (2017) Rescue of ATXN3 neuronal toxicity in *Caenorhabditis elegans* by chemical modification of endoplasmic reticulum stress. *Dis. Model. Mech.* **10,** 1465–1480 CrossRef Medline
10. McMillan, D. R., Gething, M. J., and Sambrook, J. (1994) The cellular response to unfolded proteins: intercompartmental signaling. *Curr. Opin. Biotechnol.* **5,** 540–545 CrossRef Medline
11. Shamu, C. E., Cox, J. S., and Walter, P. (1994) The unfolded-protein-response pathway in yeast. *Trends Cell Biol.* **4,** 56–60 CrossRef Medline
12. Menzies, F. M., Fleming, A., Caricasole, A., Bento, C. F., Andrews, S. P., Ashkenazi, A., Füllgrabe, J., Jackson, A., Jimenez Sanchez, M., Karabiyik, C., Licitra, F., Lopez Ramirez, A., Pavel, M., Puri, C., Renna, M., *et al.* (2017) Autophagy and neurodegeneration: pathogenic mechanisms and therapeutic opportunities. *Neuron* **93,** 1015–1034 CrossRef Medline
13. Cai, Y., Arikkath, J., Yang, L., Guo, M. L., Periyasamy, P., and Buch, S. (2016) Interplay of endoplasmic reticulum stress and autophagy in neurodegenerative disorders. *Autophagy* **12,** 225–244 CrossRef Medline
14. Vidal, R. L., and Hetz, C. (2012) Crosstalk between the UPR and autophagy pathway contributes to handling cellular stress in neurodegenerative disease. *Autophagy* **8,** 970–972 CrossRef Medline
15. Garcia-Huerta, P., Troncoso-Escudero, P., Jerez, C., Hetz, C., and Vidal, R. L. (2016) The intersection between growth factors, autophagy and ER stress: a new target to treat neurodegenerative diseases? *Brain Res.* **1649,** 173–180 CrossRef Medline

16. Bailly, C., Donkor, I. O., Gentle, D., Thornalley, M., and Waring, M. J. (1994) Sequence-selective binding to DNA of cis- and trans-butamidine analogues of the anti-*Pneumocystis carinii* pneumonia drug pentamidine. *Mol. Pharmacol.* **46,** 313–322 Medline
17. Tanious, F. A., Wilson, W. D., Patrick, D. A., Tidwell, R. R., Colson, P., Houssier, C., Tardy, C., and Bailly, C. (2001) Sequence-dependent binding of bis-amidine carbazole dications to DNA. *Eur. J. Biochem.* **268,** 3455–3464 CrossRef Medline
18. Wong, C. H., Nguyen, L., Peh, J., Luu, L. M., Sanchez, J. S., Richardson, S. L., Tuccinardi, T., Tsoi, H., Chan, W. Y., Chan, H. Y., Baranger, A. M., Hergenrother, P. J., and Zimmerman, S. C. (2014) Targeting toxic RNAs that cause myotonic dystrophy type 1 (DM1) with a bisamidinium inhibitor. *J. Am. Chem. Soc.* **136,** 6355–6361 CrossRef Medline
19. Nguyen, L., Lee, J., Wong, C. H., and Zimmerman, S. C. (2014) Small molecules that target the toxic RNA in myotonic dystrophy type 2. *ChemMedChem* **9,** 2455–2462 CrossRef Medline
20. Chan, W. M., Tsoi, H., Wu, C. C., Wong, C. H., Cheng, T. C., Li, H. Y., Lau, K. F., Shaw, P. C., Perrimon, N., and Chan, H. Y. (2011) Expanded polyglutamine domain possesses nuclear export activity which modulates subcellular localization and toxicity of polyQ disease protein via exportin-1. *Hum. Mol. Genet.* **20,** 1738–1750 CrossRef Medline
21. Bañez-Coronel, M., Porta, S., Kagerbauer, B., Mateu-Huertas, E., Pantano, L., Ferrer, I., Guzmán, M., Estivill, X., and Martí, E. (2012) A pathogenic mechanism in Huntington's disease involves small CAG-repeated RNAs with neurotoxic activity. *PLoS Genet.* **8,** e1002481 CrossRef Medline
22. Tsoi, H., Lau, C. K., Lau, K. F., and Chan, H. Y. (2011) Perturbation of U2AF65/NXF1-mediated RNA nuclear export enhances RNA toxicity in polyQ diseases. *Hum. Mol. Genet.* **20,** 3787–3797 CrossRef Medline
23. Li, L. B., Yu, Z., Teng, X., and Bonini, N. M. (2008) RNA toxicity is a component of ataxin-3 degeneration in *Drosophila*. *Nature* **453,** 1107–1111 CrossRef Medline
24. Hazeki, N., Tukamoto, T., Goto, J., and Kanazawa, I. (2000) Formic acid dissolves aggregates of an N-terminal huntingtin fragment containing an expanded polyglutamine tract: applying to quantification of protein components of the aggregates. *Biochem. Biophys. Res. Commun.* **277,** 386–393 CrossRef Medline
25. Paulson, H. L., Das, S. S., Crino, P. B., Perez, M. K., Patel, S. C., Gotsdiner, D., Fischbeck, K. H., and Pittman, R. N. (1997) Machado-Joseph disease gene product is a cytoplasmic protein widely expressed in brain. *Ann. Neurol.* **41,** 453–462 CrossRef Medline
26. Paulson, H. L., Perez, M. K., Trottier, Y., Trojanowski, J. Q., Subramony, S. H., Das, S. S., Vig, P., Mandel, J. L., Fischbeck, K. H., and Pittman, R. N. (1997) Intranuclear inclusions of expanded polyglutamine protein in spinocerebellar ataxia type 3. *Neuron* **19,** 333–344 CrossRef Medline
27. Bennett, M. J., Huey-Tubman, K. E., Herr, A. B., West, A. P., Jr., Ross, S. A., and Bjorkman, P. J. (2002) A linear lattice model for polyglutamine in CAG-expansion diseases. *Proc. Natl. Acad. Sci. U.S.A.* **99,** 11634–11639 CrossRef Medline
28. Warrick, J. M., Morabito, L. M., Bilen, J., Gordesky-Gold, B., Faust, L. Z., Paulson, H. L., and Bonini, N. M. (2005) Ataxin-3 suppresses polyglutamine neurodegeneration in *Drosophila* by a ubiquitin-associated mechanism. *Mol. Cell* **18,** 37–48 CrossRef Medline
29. Rubinsztein, D. C. (2006) The roles of intracellular protein-degradation pathways in neurodegeneration. *Nature* **443,** 780–786 CrossRef Medline
30. Yang, Y. P., Hu, L. F., Zheng, H. F., Mao, C. J., Hu, W. D., Xiong, K. P., Wang, F., and Liu, C. F. (2013) Application and interpretation of current autophagy inhibitors and activators. *Acta Pharmacol. Sin.* **34,** 625–635 CrossRef Medline
31. Gardner, B. M., Pincus, D., Gotthardt, K., Gallagher, C. M., and Walter, P. (2013) Endoplasmic reticulum stress sensing in the unfolded protein response. *Cold Spring Harb. Perspect. Biol.* **5,** a013169 Medline
32. Wang, M., Wey, S., Zhang, Y., Ye, R., and Lee, A. S. (2009) Role of the unfolded protein response regulator GRP78/BiP in development, cancer, and neurological disorders. *Antioxid. Redox Signal.* **11,** 2307–2316 CrossRef Medline
33. Lajoie, P., and Snapp, E. L. (2011) Changes in BiP availability reveal hypersensitivity to acute endoplasmic reticulum stress in cells expressing mutant huntingtin. *J. Cell Sci.* **124,** 3332–3343 CrossRef Medline
34. Pedersen, J. T., and Heegaard, N. H. (2013) Analysis of protein aggregation in neurodegenerative disease. *Anal. Chem.* **85,** 4215–4227 CrossRef Medline
35. Takahashi, T., Katada, S., and Onodera, O. (2010) Polyglutamine diseases: where does toxicity come from? what is toxicity? where are we going? *J Mol. Cell. Biol.* **2,** 180–191 CrossRef Medline
36. Lee, S. J., Lim, H. S., Masliah, E., and Lee, H. J. (2011) Protein aggregate spreading in neurodegenerative diseases: problems and perspectives. *Neurosci. Res.* **70,** 339–348 CrossRef Medline
37. Vitalis, A., Lyle, N., and Pappu, R. V. (2009) Thermodynamics of β-sheet formation in polyglutamine. *Biophys. J.* **97,** 303–311 CrossRef Medline
38. Kim, M. (2013) Beta conformation of polyglutamine track revealed by a crystal structure of Huntingtin N-terminal region with insertion of three histidine residues. *Prion* **7,** 221–228 CrossRef Medline
39. Rubinsztein, D. C., Gestwicki, J. E., Murphy, L. O., and Klionsky, D. J. (2007) Potential therapeutic applications of autophagy. *Nat. Rev. Drug Discov.* **6,** 304–312 CrossRef Medline
40. Ravikumar, B., Duden, R., and Rubinsztein, D. C. (2002) Aggregate-prone proteins with polyglutamine and polyalanine expansions are degraded by autophagy. *Hum. Mol. Genet.* **11,** 1107–1117 CrossRef Medline
41. Yamamoto, A., Cremona, M. L., and Rothman, J. E. (2006) Autophagy-mediated clearance of huntingtin aggregates triggered by the insulin-signaling pathway. *J. Cell Biol.* **172,** 719–731 CrossRef Medline
42. Arrasate, M., Mitra, S., Schweitzer, E. S., Segal, M. R., and Finkbeiner, S. (2004) Inclusion body formation reduces levels of mutant huntingtin and the risk of neuronal death. *Nature* **431,** 805–810 CrossRef Medline
43. Tanaka, M., Kim, Y. M., Lee, G., Junn, E., Iwatsubo, T., and Mouradian, M. M. (2004) Aggresomes formed by α-synuclein and synphilin-1 are cytoprotective. *J. Biol. Chem.* **279,** 4625–4631 CrossRef Medline
44. Hands, S. L., and Wyttenbach, A. (2010) Neurotoxic protein oligomerisation associated with polyglutamine diseases. *Acta Neuropathol.* **120,** 419–437 CrossRef Medline
45. Berger, Z., Ravikumar, B., Menzies, F. M., Oroz, L. G., Underwood, B. R., Pangalos, M. N., Schmitt, I., Wullner, U., Evert, B. O., O'Kane, C. J., and Rubinsztein, D. C. (2006) Rapamycin alleviates toxicity of different aggregate-prone proteins. *Hum. Mol. Genet.* **15,** 433–442 CrossRef Medline
46. Wang, T., Lao, U., and Edgar, B. A. (2009) TOR-mediated autophagy regulates cell death in *Drosophila* neurodegenerative disease. *J. Cell Biol.* **186,** 703–711 CrossRef Medline
47. Sarkar, S., Ravikumar, B., Floto, R. A., and Rubinsztein, D. C. (2009) Rapamycin and mTOR-independent autophagy inducers ameliorate toxicity of polyglutamine-expanded huntingtin and related proteinopathies. *Cell Death Differ.* **16,** 46–56 CrossRef Medline
48. Singh, V., Deepak, R. N. V. K., Sengupta, B., Joshi, A. S., Fan, H., Sen, P., and Thakur, A. K. (2018) Calmidazolium chloride and its complex with serum albumin prevent Huntingtin exon1 aggregation. *Mol. Pharm.* **15,** 3356–3368 CrossRef Medline
49. El-Ami, T., Moll, L., Carvalhal Marques, F., Volovik, Y., Reuveni, H., and Cohen, E. (2014) A novel inhibitor of the insulin/IGF signaling pathway protects from age-onset, neurodegeneration-linked proteotoxicity. *Aging Cell* **13,** 165–174 CrossRef Medline
50. Li, M., Yasumura, D., Ma, A. A., Matthes, M. T., Yang, H., Nielson, G., Huang, Y., Szoka, F. C., Lavail, M. M., and Diamond, M. I. (2013) Intravitreal administration of HA-1077, a ROCK inhibitor, improves retinal function in a mouse model of huntington disease. *PLoS ONE* **8,** e56026 CrossRef Medline
51. Ding, Y., Adachi, H., Katsuno, M., Sahashi, K., Kondo, N., Iida, M., Tohnai, G., Nakatsuji, H., and Sobue, G. (2016) BIIB021, a synthetic Hsp90 inhibitor, induces mutant ataxin-1 degradation through the activation of heat shock factor 1. *Neuroscience* **327,** 20–31 CrossRef Medline
52. Shekhar, S., Vatsa, N., Kumar, V., Singh, B. K., Jamal, I., Sharma, A., and Jana, N. R. (2017) Topoisomerase 1 inhibitor topotecan delays the disease progression in a mouse model of Huntington's disease. *Hum. Mol. Genet.* **26,** 420–429 Medline
53. Shin, B. H., Lim, Y., Oh, H. J., Park, S. M., Lee, S. K., Ahnn, J., Kim, D. H., Song, W. K., Kwak, T. H., and Park, W. J. (2013) Pharmacological activation of Sirt1 ameliorates polyglutamine-induced toxicity through the regulation of autophagy. *PLoS ONE* **8,** e64953 CrossRef Medline

54. Hsieh, C. H., Lee, L. C., Leong, W. Y., Yang, T. C., Yao, C. F., and Fang, K. (2016) A triazole derivative elicits autophagic clearance of polyglutamine aggregation in neuronal cells. *Drug Des. Devel. Ther.* **10,** 2947–2957 CrossRef Medline
55. Nagai, Y., Tucker, T., Ren, H., Kenan, D. J., Henderson, B. S., Keene, J. D., Strittmatter, W. J., and Burke, J. R. (2000) Inhibition of polyglutamine protein aggregation and cell death by novel peptides identified by phage display screening. *J. Biol. Chem.* **275,** 10437–10442 CrossRef Medline
56. Nagai, Y., Fujikake, N., Ohno, K., Higashiyama, H., Popiel, H. A., Rahadian, J., Yamaguchi, M., Strittmatter, W. J., Burke, J. R., and Toda, T. (2003) Prevention of polyglutamine oligomerization and neurodegeneration by the peptide inhibitor QBP1 in Drosophila. *Hum. Mol. Genet.* **12,** 1253–1259 CrossRef Medline
57. Nagai, Y., Inui, T., Popiel, H. A., Fujikake, N., Hasegawa, K., Urade, Y., Goto, Y., Naiki, H., and Toda, T. (2007) A toxic monomeric conformer of the polyglutamine protein. *Nat. Struct. Mol. Biol.* **14,** 332–340 CrossRef Medline
58. Zhang, Q., Tsoi, H., Peng, S., Li, P. P., Lau, K. F., Rudnicki, D. D., Ngo, J. C., and Chan, H. Y. (2016) Assessing a peptidylic inhibitor-based therapeutic approach that simultaneously suppresses polyglutamine RNA- and protein-mediated toxicities in patient cells and *Drosophila*. *Dis. Model. Mech.* **9,** 321–334 CrossRef Medline
59. Zhang, Q., Yang, M., Sørensen, K. K., Madsen, C. S., Boesen, J. T., An, Y., Peng, S. H., Wei, Y., Wang, Q., Jensen, K. J., Zuo, Z., Chan, H. Y. E., and Ngo, J. C. K. (2017) A brain-targeting lipidated peptide for neutralizing RNA-mediated toxicity in polyglutamine diseases. *Sci. Rep.* **7,** 12077 CrossRef Medline
60. Zhang, Q., Chen, Z. S., An, Y., Liu, H., Hou, Y., Li, W., Lau, K. F., Koon, A. C., Ngo, J. C. K., and Chan, H. Y. E. (2018) A peptidylic inhibitor for neutralizing expanded CAG RNA-induced nucleolar stress in polyglutamine diseases. *RNA* **24,** 486–498 CrossRef Medline
61. Liu, H., Wang, L., Lv, M., Pei, R., Li, P., Pei, Z., Wang, Y., Su, W., and Xie, X. Q. (2014) AlzPlatform: an Alzheimer's disease domain-specific chemogenomics knowledgebase for polypharmacology and target identification research. *J. Chem. Inf. Model.* **54,** 1050–1060 CrossRef Medline
62. Tsoi, H., Lau, T. C., Tsang, S. Y., Lau, K. F., and Chan, H. Y. (2012) CAG expansion induces nucleolar stress in polyglutamine diseases. *Proc. Natl. Acad. Sci. U.S.A.* **109,** 13428–13433 CrossRef Medline
63. Darrow, M. C., Sergeeva, O. A., Isas, J. M., Galaz-Montoya, J. G., King, J. A., Langen, R., Schmid, M. F., and Chiu, W. (2015) Structural mechanisms of mutant Huntingtin aggregation suppression by the synthetic Chaperonin-like CCT5 complex explained by cryoelectron tomography. *J. Biol. Chem.* **290,** 17451–17461 CrossRef Medline